Analysis of a High Temperature Supercritical Brayton Cycle for Space Exploration

Ian M. Rousseau

under the direction of
Professor Michael Driscoll
Massachusetts Institute of Technology
Nuclear Engineering Department

Research Science Institute
July 31, 2007

Abstract

This paper provides a preliminary analysis of the supercritical Brayton cycle, a power generation system for space exploration. Supercritical working fluids increase efficiency due to increased compressibility at the critical point but have not been investigated at the high temperatures necessary for space power generation. Through computer simulation, the viability of the supercritical Brayton cycle is verified for space exploration. Several working fluids are evaluated. Results show efficiency increases of 221% over the sodium Rankine cycle and 105% over thermoelectric conversion. For future cycles at 1600 K, sulfur is the best working fluid. Given present materials constraints, iodine is the best fluid at 1200 K.

1 Introduction

The purpose of this paper is to perform a preliminary analysis of high temperature supercritical Brayton cycles as it pertains to space exploration. Simple Brayton cycles have been explored for space exploration, but they are not as efficient as condensing cycles. Since supercritical fluids have properties of both liquids and gases, performing compression around the critical point increases efficiency. Supercritical Brayton cycles have been designed at an operating temperature of 650 K, but the concept has not carried over to space exploration, which requires temperatures over 1000 K. This paper provides a thermodynamic preliminary analysis of several supercritical working fluids and proves the viability of the supercritical Brayton cycle for space exploration.

1.1 Background

Humans have walked on the moon and sights are now set on manned Mars exploration, but physiological limitations of the human body in zero gravity prohibit prolonged space missions. Current travel time to Mars with conventional propulsion is at a minimum of nine months each way. In order to shorten travel time to three months, manned Mars exploration requires spacecraft velocities ranging from 40 to 100 km/second. Conventional chemical rockets will not be able to power manned missions at these velocities [9].

Electric ion propulsion is a promising propulsion system for future space exploration. An electric field charges and ejects atoms of a noble gas (xenon or krypton). A 25 kW prototype of an electric xenon ion system achieved more than fifteen times the efficiency of today's best chemical rockets [21]. To go to Mars and beyond, 100-400 kW thrusters are needed [25].

Currently, there is no way to fulfill an electric ion thrusters' power requirements in space. Solar cell arrays are heavy and would not receive enough sunlight in deep space. A small nuclear fission reactor (less than 1 MW) would meet this power requirement, but reactor thermal energy needs to be processed by power converters to create electric power.

There are two methods to extract electrical energy from the thermal energy of nuclear reactions. *Static conversion* uses no moving parts to generate DC power. This method is ideally suited for space flight because the absence of moving parts negates the possibility of mechanical failure. However, static conversion methods are currently limited in total power output, efficiency, and mass. Thermionic converters, thermophotovoltaic cells, and thermoelectric converters are examples of static conversion [1].

Dynamic power conversion (heat cycles) converts thermal energy into AC power. Thermal energy is transferred to a working fluid. The fluid is compressed and heated before being sent through a turbine, which is linked to a generator. Although dynamic conversion may be more complex than static methods, heat cycles are scalable and the technology is mature; coal, nuclear, wood, and gas powerplants use heat cycles. Dynamic power conversion methods include the Stirling, Rankine, Carnot, Otto, and Brayton cycles [2]. Of these, only the Brayton cycle is ideally suited for space because its simplicity decreases the likelihood of mechanical failure.

Simple Brayton cycles function much like closed circuit jet engines with near-ideal gases. First, the gas is compressed via a compressor linked to the turbine. Next, heat is added to increase gas enthalpy. The hot, high pressure gas is sent through a turbine to generate electricity. Finally, the gas releases thermal energy in the radiator before beginning the cycle again (Figure 1; See Appendix A). A helium Brayton cycle for terrestrial power plants achieved 43% efficiency at 1073 K [8]. By comparison, today's best coal power plants are 35-40% efficient [17].

Heat cycles in space present a major difficulty. Since there is no matter in space, radiation is the sole option for releasing thermal energy. The gray body heat radiation, Q_{rej}, is defined

[1]Information about static converison methods can be found in Appendix B.

[2]See [3] for information about heat cycles.

as follows [3]:

$$Q_{rej} = \sigma \epsilon A T_r^4 \tag{1}$$

where σ is the Steffan-Boltzmann constant ($5.76*10^{-8}$ W/m^{2}K^4), ϵ is surface emissivity, A is radiator area (m^2), and T_r is the radiator temperature (K). Since Q_{rej} is fourth order with respect to T_r, high radiator temperatures are favored.

These high radiator temperatures present a major problem for the Brayton cycle. The maximum efficiency for a given cycle with maximum temperature T_3 and minimum temperature T_1 is the Carnot efficiency, η defined as:

$$\eta = \frac{T_3 - T_1}{T_3} \tag{2}$$

Efficiency can be increased through the addition of recuperators (preheaters). In space, this option is not practical because of the high cost of launching payloads ($50847/kg for the Space Shuttle in 2000 [13]). Radiator size indicates total system mass. Hence, specific power, or power output per unit radiator area, was optimized.

A Supercritical Carbon Dioxide Cycle for Next Generation Nuclear Reactors [8] has delivered promising results for increasing Brayton cycle efficiency without increasing mass. If a working fluid is compressed near its critical point, compressor work decreases up to 75% [6]. A Brayton cycle using supercritical carbon dioxide at 823 K was demonstrated to have the same efficiency as a ideal helium system at 1073 K. These cycles were designed for power plants and contain intercoolers and recuperators [8], and the concept has not yet been applied to space flight.

This paper focuses on the development of a Brayton cycle nuclear engine for space exploration. The temperature limit for current materials is 1200 K. In order to enable development in the near future, high cycle temperatures did not exceed 1600 K and the SAFE-400 reactor

[3] The temperature of outer space, 0 K, can be neglected in these calculations.

was used. The SAFE-400, a standard reactor in theoretical nuclear spacecraft design, is a 400 kW highly enriched uranium fission reactor operating at 1250 K. Supercritical working fluids were used to increase cycle efficiency. Working fluid selection optimized power output per unit radiator area.

2 Methods and Materials

2.1 Working Fluid Selection

Working fluid selection was based on several criteria. First, the fluid's critical point must fall within a given range, 800-1400 K. If the critical temperature (T_c) is too low, radiator mass increases according to the gray body radiation equation (Equation 1). If the critical temperature is too high, efficiency and power output drop according to Carnot efficiency (Equation 2). Corrosion properties of the supercritical fluid are considered. For space missions, system reliability and low mass are the foremost goals. Exotic and expensive materials are employed in an effort to increase performance.

Table 2.1 lists properties for inorganic compounds with critical temperatures between 800 and 1400 K. Organic compounds may decompose at these temperatures and thus are not included.

Substance	Formula	T_c (K)	P_c (Pa)	C_p (J/mol-K)	$\frac{C_p}{C_v}$ (k)
Arsenic Oxide	As_2O_3	1200	$4*10^6$	22.9	1.15
Ferric Chloride	$FeCl_3$	948.15	$4.3*10^6$	82.89	1.2
Iodine	I_2	819.15	$1.1654*10^7$	38.77	1.4
Phosphorus	P	993.75	$8.3289*10^6$	20.79	1.55
Sulfur	S	1313	$1.8208*10^7$	21.21	1.3
Sulfuric Acid	H_2SO_4	924	$6.4*10^6$	137.4	1.13
Tetraphosphorus Decasulfide	P_4S_{10}	1291	$2.32*10^7$	32.272	1.1

Table 1: Supercritical fluid physical properties [5][19].

2.1.1 Supercritical Fluid Model

Supercritical fluids cannot be modeled as ideal gases around the critical point [6]. Experimental data is used to determine supercritical properties, but high temperature supercritical fluid data was unavailable. Properties of the gases were determined based on available formulas. The specific heat, C_p, was either found in a reference table [19] or calculated from a formula [5] at the average cycle temperature. The ratio of specific heats, k, is dependent on both the number of atoms per molecule and the molar mass of the fluid. A reference table was used to estimate k values [7].

To correct for real supercritical behavior, the pseudo-perfect gas model was adopted. This model approximates compression works savings through a compressibility factor, Z [1]. Z is dependent on both the reduced temperature, T_r and pressure, P_r [4]. A table of Z values was used in all calculations (see Figure 2). The compressibility chart was constant for all fluids, except when a critical compressibility factor was provided.

2.2 Thermodynamics Theory

An ideal Brayton cycle was modeled through a set of equations. The ideal calculations assume that the working fluid is an ideal gas, C_p does not vary with temperature, there are no pressure losses, and compression is adiabatic[5]. Compression factors approximate real supercritical fluid behavior.

For a given calculation, four constants are needed. First, the pressure ratio across the turbine and compressor, R_p is specified. By definition, a Brayton cycle is non-condensing. Therefore, the minimum cycle temperature and operating pressure, T_1 and P_1 must be greater than or equal to the critical point. Finally, T_3 is specified. In these simulations, T_3 is less than or equal to 1600 K due to materials constraints. From these values, cycle operation

[4]Ratio of current temperature to critical temperature and current pressure to critical pressure

[5]No heat is gained from or lost to the surrounding environment.

parameters are calculated.

The Brayton cycle's power output is the difference between the turbine and compressor work. Turbine work is equal to the difference in enthalpy of the fluid before and after compression (see Figure 3). To find the work, the compressor and turbine inlet and outlet temperatures must be calculated.

$$\frac{T_2}{T_1} = \frac{T_3}{T_4} = R_p^{\frac{k-1}{k}} \tag{3}$$

Ideal gas Brayton cycle efficiency is given by the following expression:

$$\eta_{ideal} = 1 - R_p^{\frac{k}{1-k}} \tag{4}$$

Compressor work per unit mass flow (specific work) is defined below:

$$w_c = \frac{1}{\eta_c} C_p (Z_2 T_2 - Z_1 T_1) \tag{5}$$

where η_c is the compressor efficiency (assumed to be 0.90 [24]). Turbine specific work is

$$w_t = \eta_t C_p (Z_3 T_3 - Z_4 T_4) \tag{6}$$

where η_t is the turbine efficiency (assumed to be 0.90 [24]). Z_n is the compressibility factor at T_n. q_{in} is the specific work added to the cycle from the reactor, given by:

$$q_{in} = C_p (Z_3 T_3 - Z_2 T_2) \tag{7}$$

The net specific work, w_{net} is the difference between the turbine and compressor specific work. The cycle's real gas efficiency is then

$$\eta_{real} = w_{net}/q_{in} \tag{8}$$

The output work is defined as:

$$W_{out} = \eta_{real} Q_{in} \tag{9}$$

where Q_{in} is the energy output of the reactor. Q_{in} was assumed to be 80% of full reactor power, or 360 kW, to compensate for real Brayton cycle losses. According to the First Law of Thermodynamics, energy is conserved.

$$Q_{in} = W_{out} + Q_{rej} \tag{10}$$

Rather than taking the average of T_1 and T_4 to calculate radiator size, Equation 1 is integrated from T_4 to T_1 to improve accuracy [3].

$$Q_{rej} = \frac{1}{T_4 - T_1} \int_{T_4}^{T_1} \sigma \epsilon A T^4 dT \tag{11}$$

2.3 Computer Simulation

The Brayton cycle was modeled in a computer simulation programmed in Java. By using a computer simulation, multiple iterations can be quickly calculated. Results are recorded in a text file, enabling spreadsheet analysis. The user is able to specify fluid, pressure, and temperature parameters. A library of fluids was added for convenience. Different working fluids were compared quantitatively.

The program prompts the user to either select the working fluid from the library or generate a new properties file. If a new properties file is generated, it is stored in the library for future use. Then, the user is asked to input T_1, T_3, P_1, and the simulation step size. The simulation increments the pressure ratio by the step size until a maximum pressure ratio is reached (5 in these simulations), performing calculations at each step. The calculations are recorded in a formatted text file.

Since the compressibility table contains no formula for calculating intermediate values, an estimation algorithm had to be adopted. Global regressions generalize local extrema, and were discarded. The table was in three dimensions, further complicating calculations. To estimate intermediate values, the four vertices around the point were found. Two linear regressions were performed at constant pressure. These two points were used to perform a linear regression at constant temperature, yielding a compressibility value.

3 Results

Simulations were run at two temperatures. High temperature (1600 K) simulations were run for each fluid to simulate potential future Brayton cycles. 1200 K tests were run to simulate supercritical Brayton cycles that could be implemented today. 1200 K is close to the heat pipe outlet temperature of the SAFE-400 reactor, 1250 K [14]. The 1600 K cycle would require a higher outlet temperature reactor. Fluids not included in the 1200 K simulations did not produce cycles with positive work output. In the tables,"I" refers to ideal gas efficiency, while "R" refers to compressibility corrected efficiency. All other calculations are for corrected gas behavior. Table values were optimum specific power values for each fluid. If the specific power calculation diverged, optimum specific work values were chosen. If specific work diverged, then the calculation with an pressure ratio of 2.25 was selected.

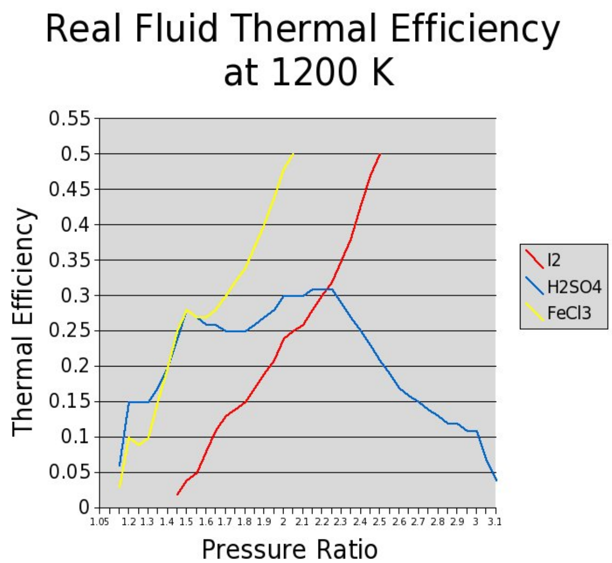
Real Fluid Thermal Efficiency at 1200 K
Thermal Efficiency
Pressure Ratio
I2
H2SO4
FeCl3

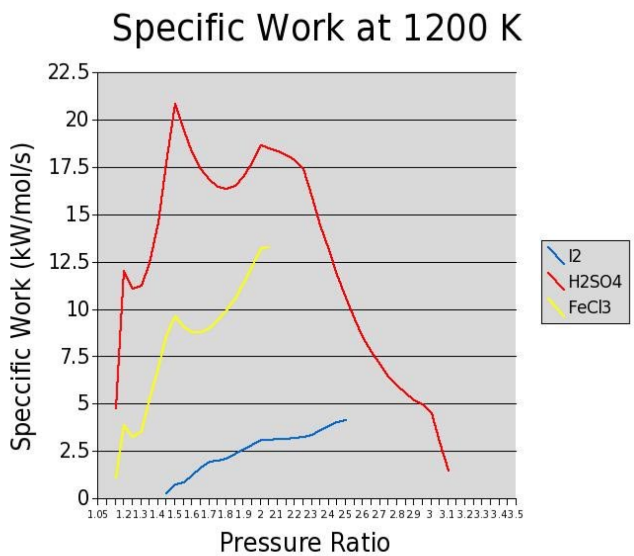
Specific Work at 1200 K
Speccific Work (kW/mol/s)
Pressure Ratio
I2
H2SO4
FeCl3

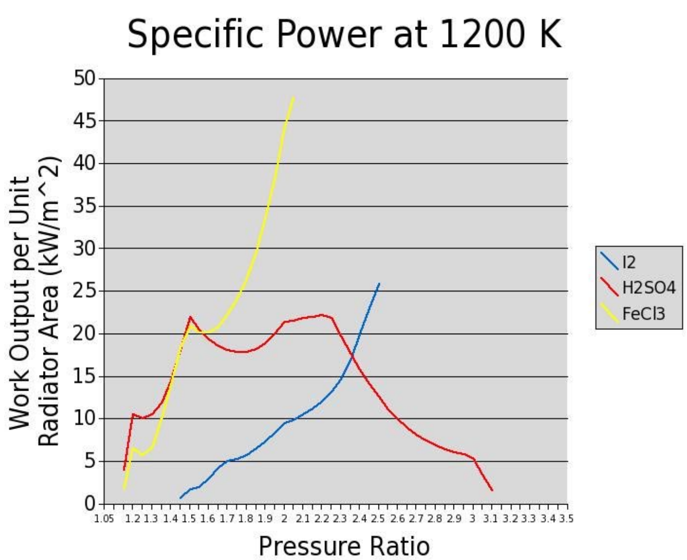
Specific Power at 1200 K
Work Output per Unit Radiator Area (kW/m^2)
Pressure Ratio
I2
H2SO4
FeCl3

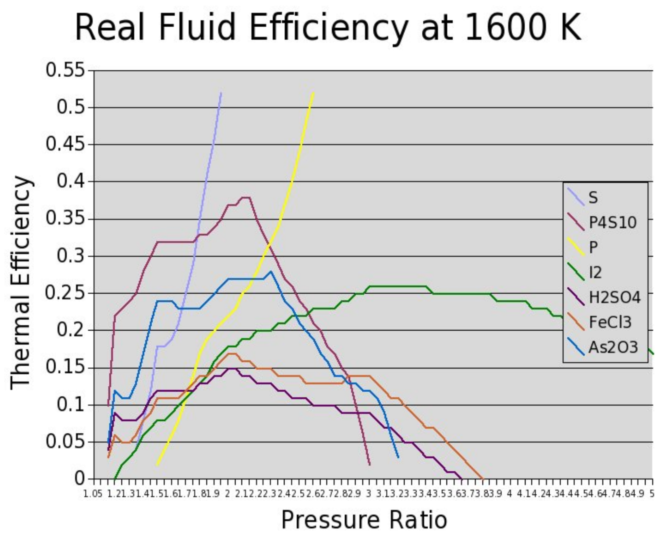

Real Fluid Efficiency at 1600 K
Thermal Efficiency
Pressure Ratio
S
P4S10
P
I2
H2SO4
FeCl3
As2O3

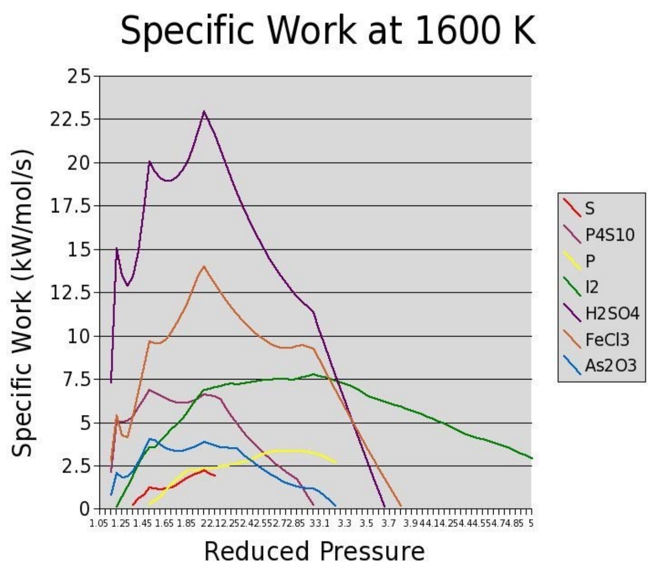

Specific Work at 1600 K
Specific Work (kW/mol/s)
Reduced Pressure
S
P4S10
P
I2
H2SO4
FeCl3
As2O3

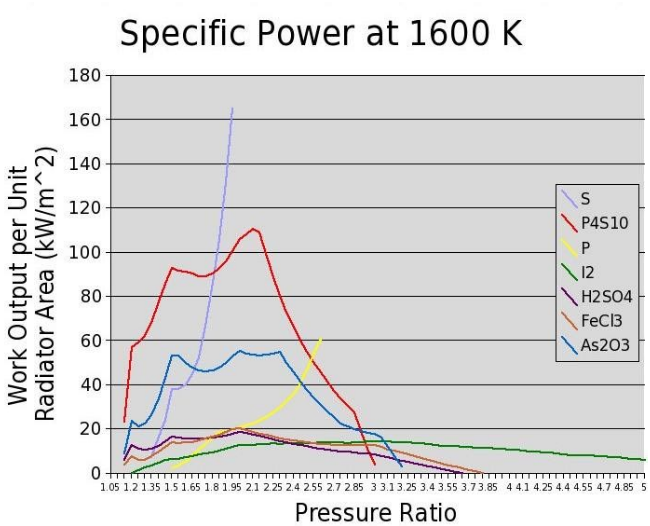

Specific Power at 1600 K
Work Output per Unit Radiator Area (kW/m^2)
Pressure Ratio
S
P4S10
P
I2
H2SO4
FeCl3
As2O3

Fluid	R_p	Eff. (I)	Eff. (R)	Power (kW)	Specific Work ($\frac{kW-s}{mol}$)	Specific Power ($\frac{kW}{m^2}$)
$FeCl_3$	2.25	0.13	0.55	196.2	12.43	55.63
H_2SO_4	2.20	0.09	0.31	111.3	45.2	22.22
I_2	2.25	0.21	0.32	115.5	3.32	13.24

Table 2: Performance at 1200 K

Fluid	R_p	Eff. (I)	Eff. (R)	Power (kW)	Specific Work ($\frac{kW-s}{mol}$)	Specific Power ($\frac{kW}{m^2}$)
As_2O_3	2.00	0.09	0.27	97.3	3.94	55.63
$FeCl_3$	2.00	0.11	0.17	61.3	14.02	20.45
H_2SO_4	2.00	0.08	0.15	53.8	22.97	18.97
I_2	3.00	0.27	0.26	92.0	7.81	15.37
P	2.50	0.28	0.44	158.8	3.11	46.54
P_4S_{10}	2.10	0.07	0.38	136.8	6.57	110.58
S	2.00	0.15	0.59	210.8	2.28	210.02

Table 3: Performance at 1600 K

4 Discussion

In order to provide a point of comparison, Yarsky *et al.* achieved 19% thermal efficiency with an ideal Brayton cycle at 1400 K [24] and 12% efficiency with a sodium Rankine cycle at 1400 K. Real fluid efficiency was greater than ideal fluid efficiency in all cases except for I_2 at 1600 K. I_2 had a ΔT at 1600 K. Thus, the reduced temperature T_{r2} corresponded to a Z near one. Fluids with critical points near maximum operating temperature generally had higher efficiencies than fluids with high ΔT values because T_2 was closer to the critical point. Selected values' R_p ranged from 2 to 3, indicating the optimum pressure ratio for a 1600 K space power system falls within this range. High efficiency and low specific work implied high values of $\dot{m}$. Specific power seemed to be exponentially related to ΔT. Efficiency diverged for I_2 (1200 K), S (1600 K), P (1600 K), and $FeCl_3$ (1200 K). These three substances have the highest k values, (1.2-1.6). Large k values contributed to divergence by increasing T_2 and decreasing T_4.

The best fluid for the 1200 K cycle was I_2. H_2SO_4 had the highest specific net work because it also has the greatest C_p, but it fell behind $FeCl_3$ and I_2 in both efficiency and specific power at pressure ratios greater than 2.4. While $FeCl_3$'s performance in all categories exceeded I_2's performance, its melting point is 577 K. I_2's melting point[5] is 387 K. The working fluid must be in the liquid state at launch to avoid system damage. The reactor won't be started until orbit is reached, so a separate heat source is needed. I_2 would require a smaller heat source and was therefore the best choice.

For the 1600 K cycle, the best working fluid was sulfur. Sulfur had the highest specific power and thermal efficiency at lower pressure ratios than other fluids. Its main drawback was low specific work, implicating an $\dot{m}$ of 92.53 mol/s, as compared to P_4S_{10}'s $\dot{m}$ of 20.82 mol/s. Heat source weight reduction during launch was the last topic for consideration. Phosphorous (white) has a melting point of 317 K, while sulfur's melting point is 387 K. Sulfur is the better fluid because it had higher specific power at lower pressure ratios.

4.1 Design Weaknesses

Operating pressures greater than 10^7 Pa imply that pipe mass must increase to compensate for the increased pressure. For thin-walled pipes, pipe mass to confine a given mass of fluid is constant with pressure [6] [22] [10]. Without knowing total pipe length in each system, no comparison was possible. Since the increased efficiency of the supercritical Brayton cycle allows higher radiator temperatures, supercritical system radiator mass is less than both the sodium Rankine cycle and conventional Brayton cycle radiator mass. The working fluids in the supercritical Brayton cycle had higher atomic mass than either the sodium Rankine or supercritical carbon dioxide cycles (89.13 g/mol for $S_2.78$ and 253.8 g/mol for I_2 versus 22.99 g/mol for Na and 44.01 g/mol for CO_2). Increased molecular mass decreased turbine and compressor size [24].

[6] For a full derivation, see Appendix C

Special materials have to be considered for construction of this high temperature Brayton cycle. There are three options for materials: refractory metals, ceramic coatings, and oxide strengthened steels. Materials must avoid corrosion at these temperatures. Exotic ceramic coatings, such as TaN, B_4C, HfC, ZrN, BN, or HfN can withstand operating temperatures greater than 1000 K [15]. Refractory metals such as columbium, molybdenum, tantalum, tungsten, and their alloys display oxidation resistance at temperatures greater than 1000 K [16]. Oxide strengthened steels are capable of withstanding these temperatures, but corrosion compatibilities with supercritical I_2 and S need to be determined. Some combination of these substances may yield a satisfactory working material.

Objections will be raised about the use of toxic chemicals as working fluids. At high temperatures, however, any material is dangerous. For example, supercritical steam is extremely corrosive at 800 K. Citing precedent, H_2SO_4, I_2, and S are currently used for large scale hydrogen production at 1273 K. Plutonium has already been launched into orbit for the Cassini mission [20]. The SAFE-400, a highly enriched uranium reactor, will not be started until it is in orbit. With the reliability of today's launch vehicles, risk is mitigated. Since operation is in space, a pressure leak will pose no threat to the environment.

5 Conclusions

The pseudo-perfect gas model (Law of Corresponding States) proves the viability of the supercritical Brayton cycle based on both efficiency and weight reduction. At 1600 K, the best working fluid is sulfur. If limited by current materials constraints at 1200 K, the best working fluid is I_2. High temperature supercritical Brayton cycles deserve further theoretical and experimental research.

5.1 Further Work

The simulation needs improvement to more closely model real supercritical fluids and a real Brayton cycle. The next step is use of generalized enthalpy and entropy charts instead of compressibility values. Since a real Brayton cycle is not isothermal, using constant C_p is an approximation. For I_2, C_p increases by 1.7% on the temperature interval from 800 K to 1200 K and 5.9% between 800 K and 1600 K. Ideal Brayton cycle equations must be integrated over the operational temperature range to estimate the real Brayton cycle. A method for estimating total system mass must be adopted.

Physical properties of high temperature supercritical fluids must be experimentally measured. These measurements should provide the basis for a supercritical fluid model. Corrosion properties of working fluids at these high temperatures should be determined. Many working fluids, such as sulfur and phosphorus, have unique properties that may alter physical and corrosion properties at temperatures greater than 1000 K. Sulfur gas is a mixture of S_8, S_7, S_6, S_5, S_4, S_3, S_2, and S_1. At the critical point, there are 2.78 atoms per molecule [5]. With increasing temperature, this number decreases [18]. Phosphorus has three allotropes, red, white, and black phosphorus. The melting point of red phophorus is 870 K, while the melting point of white phosphorus is 317 K. White phosphorus is much more reactive than either red or black phosphorus. Allotrope abundance in supercritical fluids is unknown.

Current materials constraints limit maximum cycle temperature to 1200 K [19]. New materials should be developed to withstand high temperatures, possibly allowing high cycle temperatures up to 1600 K. Additionally, eutectics, mixtures of fluids, could provide working fluids with intermediate properties. A pressure leak in a space heat cycle would be catastrophic. Small diameter heat pipes could be used to increase robustness. A heat pipe uses capillary action to move fluids. Heat pipe performance in zero gravity environments and with supercritical fluids needs to be studied [26] [9].

6 Acknowledgments

I am indebted to the Center for Excellence in Education for providing me with the opportunity to attend RSI 2005. I would like to thank my sponsors, Mr. Raymond Kubacki, Mr. Peter Muller, Dr. Gerry Rossi, and Mr. and Mrs. Robert G. Stern, for their support. I am grateful for Dr. Jenny Sendova and Dr. Dennis Ugolini, who provided me with this mentorship and aided in the writing of this document.

I thank my mentor, Professor Michael Driscoll, for his guidance. Professor Driscoll always knew the answer or pointed me in the right direction to solve my questions. I am also indebted to Professor Andrew Kadak and Mr. Peter Yarsky for their input and experience in the field of nuclear power in space.

References

[1] R. H. Aungier: *Axial-Flow Compressors.* ASME Press, New York, NY (2003).

[2] W. Z. Black, J. G. Hartley. *Thermodynamics, 2nd Edition.* Harper Collins, New York, NY (1991).

[3] R. O. Buckius, J.R. Howell: *Fundamentals of Engineering Thermodynamics.* McGraw-Hill, Highstown, NJ (1992).

[4] C.J. Crowley, N.A. Elkouh. Plasma-sprayed selective emitters for thermophotovoltaics. Available at `http://www.nasatech.com/Briefs/Sept00/LEW16809.html` (2005/07/08).

[5] T.E. Daubert, R.P. Danner, J.L. Oscarson, H.M. Sibul, C.C. Stebbins, R.J. Rowley, R.L. Rowley, W.V. Wilding, Y. Yang. *Physical and Thermodynamic Properties of Pure Chemicals.* Vol. 1-5. Greyden Press, Columbus, OH (2003).

[6] P.G. Debenedetti, E. Kiran, C.J. Peters: *Supercritical Fluids: Fundamentals and Applications.* Kluwer Academic Publishers, Dordrecht, the Netherlands (1998).

[7] Michael de Podesta: *Understanding the Properties of Matter.* Taylor & Francis, London, England (1996).

[8] V. Dostal, M.J. Driscoll, P. Hejzlar: *A Supercritical Carbon Dioxide Cycle for Next Generation Nuclear Reactors.* Ph.D. thesis, Advanced Nuclear Power Technology Program, Cambridge, MA (2004).

[9] V. Dostal, K. Gezelius, J. Horng, J. Koser, J. Palaia, E. Shwageraus, P. Yarsky, A. Kadak: *Mission to Mars: How to Get There and Back with Conventional Nuclear Energy.* Massachusetts Institute of Technology, Cambridge, MA (2004).

[10] M. Driscoll, Proof of Decreasing Specific System Mass with Increasing Pressure. Unpublished manuscript (2005).

[11] K. Emery. Characterizing Thermophotovoltaic Cells. Semiconductor Science and Technology. Available at `http://www.iop.org/EJ/article/0268-1242/18/5/313/s30513.pdf` (2005/07/08).

[12] J. Esley: *Nature's Building Blocks: An A–Z Guide to the Elements.* Oxford University Press, New York, NY (2001).

[13] The Futron Corporation: *Space Transportation Costs: Trends in Price Per Pound to Orbit 1990-2000.* Available at: `www.futron.com/pdf/FutronLaunchCostWP.pdf` (2005/07/14).

[14] R. Guffee, R. Kapernick, D. Poston: *Design and Analysis of the SAFE-400 Space Fission Reactor*. Found in: *AIP Conf. Proc. 608: Space Technology and Applications International Forum*. Available at `http://scitation.aip.org/getabs/servlet/GetabsServlet?prog=normal&id=APCPCS000608000001000578000001&idtype=cvips&gifs=yes` (2005/07/13).

[15] E. Lang: *Coatings for High Temperature Applications.* CEC High Temperature Materials Information Center, the Netherlands (1983).

[16] Metallurgical Society Conferences: *Refractory Metals and their Alloys.* Interscience Publishers, New York, New York (1960).

[17] J.T. McMullan, B.C. Williams, E.P. Sloan: *Clean Coal Technologies.* Available at: `http://www.ingentaconnect.com/content/pep/jpe/1997/00000211/00000001/art00008` (2005/07/14).

[18] C. Meyer:*Elemental Sulfur.* Interscience Publishers, Inc., New York, NY (1965).

[19] National Institute of Standards and Technology: *NIST Reference Fluid Thermodynamic and Transport Properties Database.* Available at: `http://www.nist.gov/srd/nist23.htm` (2005/07/15).

[20] Office of Space Defence & Power Systems. Radioisoptope power systems. Available at `http://www.ne.doe.gov/space/space-desc.html` (2005/07/07).

[21] S. Olasen and I. Katz: *Electric Propulsion for Project Prometheus.* Presented at: *39th AIAA/ASME/SAE/ASEE Joint Propulsion Conference and Exhibit*. Available at: `http://www.aiaa.org/content.cfm?pageid=406&gTable=Paper&gID=13898` (2005/07/28).

[22] R. J. Roark: *Formulas for Stress and Strain.* McGraw-Hill, New York, NY (1943).

[23] J. Viegas. Heat wave. New Scientist 182 (2004/09/04), no 2463, 34–35.

[24] P. Yarsky, A.C. Kadak, M.J. Driscoll: *Design of a Sodium-cooled Epithermal Long-term Exploration Nuclear Engine.* M.S. Thesis, MIT Nuclear Science and Engineering Department, Cambridge, MA (2004).

[25] J.E. Polk, T.M. Randolph: *An Overview of the Nuclear Electric Xenon Ion System (NEXIS) Activity*. Found in: *Space 2004 Conference and Exhibit Proceedings*. Available at: `http://www.aiaa.org/content.cfm?pageid=406&gTable=Paper&gID=23133` (2004/07/14).

[26] L. L. Vasiliev: *Heat Pipe Technology – Volume 2: Materials and Applications*. Found in: *Proceedings of the 7th International Heat Pipe Conference.* Bergell House, 1993.

A Appendix A

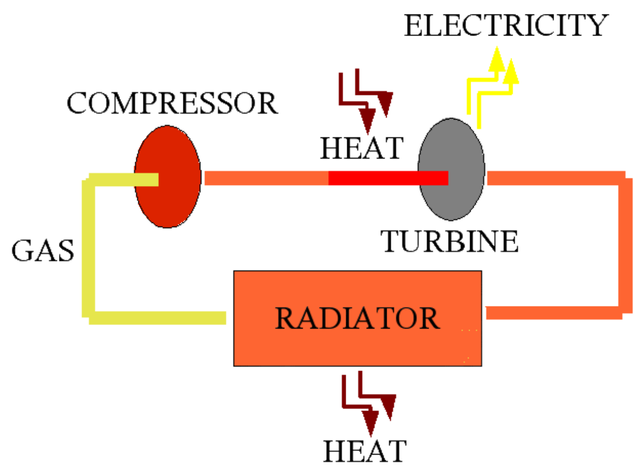

Figure 1: The Brayton cycle

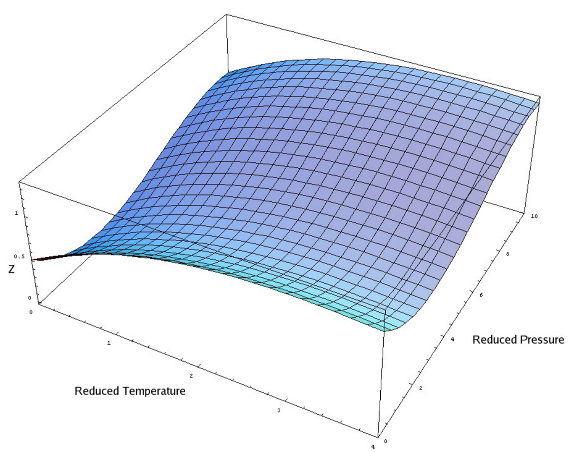

Figure 2: Z correction factors for the pseudo-perfect gas model. Note depression around the critical point

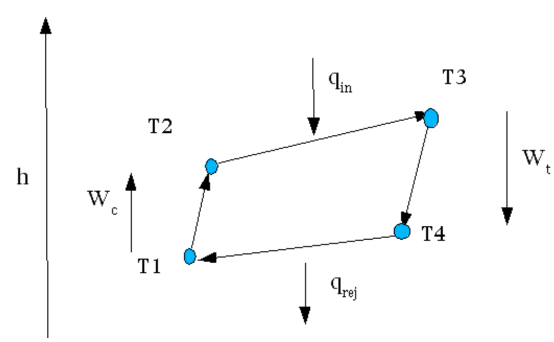

Figure 3: Brayton cycle enthalpy

B Appendix B

The three types of static conversion are thermionic (TIC), thermophotovoltaic (TPV), and thermoelectric.

Space probes such as Voyager and Cassini have used thermionic power converters (TIC). TICs use the Seebeck Effect to generate power from heat energy. Heat from radioactive decay of plutonium-238 oxide is applied to a device with p- and n-type semiconductor material, creating a potential difference between materials. While this system requires no moving parts, TICs are limited in power output; the first thermoelectric device generated just 2.7 watts, while the largest thermoelectric cell, built for the Cassini-Huygens probe, generated 290 watts [20]. TIC efficiency is proportional to temperature, and power production is proportional to the difference in temperatures between the emitter and collector. Single layer TICs have been tested experimentally, obtaining efficiencies greater than 12.4% between 750 and 1200 K. Double layer TICs, where one layer's emitter is connected to the next layer's collector, will generate approximately 2.5 times the useful work of the single layer system [24].

TPVs convert thermal to light to electrical energy. First, a substrate is heated. The substrate is coated with a thin (15-250 μm) emitter coating made of rare earth oxides. The substrate uses the photoelectric effect to emit light on selected wavelengths. These wavelengths are engineered to optimize photovoltaic cell efficiency [4]. Currently, there are few reliable efficiency figures for TPV cells because measurement criteria have not been standardized [11].

Thermoelectric converters use the Seebeck effect, like TICs, to generate electricity. Thermoelectrics are made of heavy metals, which conduct heat as well as electricity. Thus, thermoelectrics often radiate heat to the cold end of the material, degrading performance. Research has been focused on finding compounds that conduct electricity but not heat. Since 1950, the standard compound has been lead telluride (efficiency less than 10%). In 1996, MIT professors Mildred Dresselhaus and Lyndon Hicks found that a sandwich of europium lead tellride and lead telluride did not conduct heat well at the boundary. In 2004, Mercouri Kanatzidis of Michigan State University had a breakthrough. An alloy of antimony, tellurium, lead, and silver produced 18% thermal efficiency. On the nanoscale, this alloy creates "islands" of PbTe that absorb phonons and the larger "sea" of metal atoms scatters phonons. [23]

C Appendix C

From [22],

$$\sigma = \frac{Pd}{2t}$$

where σ is the hoop stress around the tube's circumference (takes on constant allowable value), P is the pressure, d is the pipe diameter, and t is the wall thickness. The mass of fluid, M_f, is given by:

$$M_f = \frac{MP}{RT}\frac{\pi}{4}d^2 * 1$$

where M is the molar mass of the fluid, R is the gas constant (8314 Pa-L/mol-K), and T is the temperature. The 1 is added to make volume per unit length. The mass of the pipe, M_p is equal to

$$M_p = \pi d t \rho_p$$

where ρ_p is the pipe density. Then it follows that the ratio between the two masses is:

$$\frac{M_f}{M_p} = \frac{4RTdt\rho_p}{MPd^2}$$

substituting back in for t yields:

$$\frac{M_f}{M_p} = \frac{2RT\rho_p}{M\sigma}$$